Mouse SYCP2 is required for synaptonemal complex assembly and chromosomal synapsis during male meiosis

Fang Yang,[1] Rabindranath De La Fuente,[2,4] N. Adrian Leu,[3,4] Claudia Baumann,[2,4] K. John McLaughlin,[3,4] and P. Jeremy Wang[1]

[1]Department of Animal Biology, School of Veterinary Medicine, University of Pennsylvania, Philadelphia, PA 19104
[2]Female Germ Cell Biology Group, Department of Clinical Studies, [3]Department of Animal Biology, and [4]Center for Animal Transgenesis and Germ Cell Research, New Bolton Center, School of Veterinary Medicine, University of Pennsylvania, Kennett Square, PA 19348

During meiosis, the arrangement of homologous chromosomes is tightly regulated by the synaptonemal complex (SC). Each SC consists of two axial/lateral elements (AEs/LEs), and numerous transverse filaments. SC protein 2 (SYCP2) and SYCP3 are integral components of AEs/LEs in mammals. We find that SYCP2 forms heterodimers with SYCP3 both in vitro and in vivo. An evolutionarily conserved coiled coil domain in SYCP2 is required for binding to SYCP3. We generated a mutant *Sycp2* allele in mice that lacks the coiled coil domain. The fertility of homozygous *Sycp2* mutant mice is sexually dimorphic; males are sterile because of a block in meiosis, whereas females are subfertile with sharply reduced litter size. *Sycp2* mutant spermatocytes exhibit failure in the formation of AEs and chromosomal synapsis. Strikingly, the mutant SYCP2 protein localizes to axial chromosomal cores in both spermatocytes and fetal oocytes, but SYCP3 does not, demonstrating that SYCP2 is a primary determinant of AEs/LEs and, thus, is required for the incorporation of SYCP3 into SCs.

Introduction

Meiosis, which is a process unique to germ cells, consists of two successive rounds of cell divisions without intervening DNA replication, and, thus, produces haploid germ cells to cope with genome doubling at fertilization. One hallmark of meiosis is the assembly and disassembly of a proteinaceous tripartite structure, the synaptonemal complex (SC), during the prophase of meiosis I (Fawcett, 1956; Moses, 1956, 1969; Page and Hawley, 2004). The SC consists of two lateral elements (LE) and a central element (CE). During the leptotene stage of prophase I, axial elements (AE) are formed along chromosomal cores between sister chromatids. During the subsequent zygotene stage, the AEs of two homologous chromosomes become connected by transverse filaments (TF) in a process referred to as synapsis. Because TFs overlap in the center to form a CE, AEs, TFs, and the CE constitute the tripartite SC. In the context of SCs, AEs are called LEs. At the pachytene stage, synapsis occurs along the entire length of homologous chromosomes, except for XY chromosomes in mammals. During the diplotene stage, SCs disassemble and homologous chromosomes are separated, except at regions of crossover, which are known as chiasmata (Page and Hawley, 2004).

Studies of meiosis-specific proteins in model organisms (e.g., Zip1, Red1, Hop1, and Mek1) have provided insights into the functions of SC (Roeder, 1997). In budding yeast, the Red1 protein localizes to AEs and is required for the formation of AEs (Smith and Roeder, 1997). Hop1 interacts with, and localizes to the same sites as, Red1, and the localization of Hop1 to AE is dependent on Red1 (Hollingsworth and Ponte, 1997; Smith and Roeder, 1997; de los Santos and Hollingsworth, 1999). Additionally, genetic studies have shown that the stoichiometry of Red1 and Hop1 is critical for AE assembly (Friedman et al., 1994; Hollingsworth and Ponte, 1997). Mek1 is a meiosis-specific serine/threonine kinase involved with the SC assembly, and it interacts with Red1 physically and genetically. Phosphorylation of Red1 is Mek1-dependent and is required for Red1–Hop1 heterooligomer formation, and, thus, is critical for the formation of the SC (Bailis and Roeder, 1998; de los Santos and Hollingsworth, 1999). Zip1 is a major component of TFs in yeast and is required for chromosomal synapsis (Sym et al., 1993). Components of TFs have been identified in *Drosophila*

Correspondence to P. Jeremy Wang: pwang@vet.upenn.edu

Abbreviations used in this paper: AE, axial element; CE, central element; dpc, days postcoitum; ES, embryonic stem; LE, lateral element; SC, synaptonemal complex; SYCP, synaptonemal complex protein; TF, transverse filament.

The online version of this article contains supplemental material.

The Journal of Cell Biology, Vol. 173, No. 4, May 22, 2006 497–507
http://www.jcb.org/cgi/doi/10.1083/jcb.200603063

melanogaster (C[3]G) and *Caenorhabditis elegans* (SYP-1 and -2; Page and Hawley, 2001; MacQueen et al., 2002; Colaiacovo et al., 2003). A common feature of TF components in these diverse organisms is that they are coiled coil proteins (Page and Hawley, 2004).

Although extensive ultrastructural studies of SCs have been performed in mammalian species such as rat and hamster (von Wettstein et al., 1984), isolation of SCs have identified the key components of mammalian SCs, including SC proteins 1, 2, and 3 (SYCP1, -2, and -3; Heyting et al., 1989; Meuwissen et al., 1992; Dobson et al., 1994; Lammers et al., 1994; Offenberg et al., 1998). SYCP1 contains coiled coils and is a major component of TFs. Despite their similar functions in meiosis, SYCP1 bears no apparent sequence similarity with TF components in other organisms, such as yeast Zip1, fly C(3)G, and nematode SYP-1 and -2, other than them all being coiled coil proteins. Recently, two SYCP1-interacting proteins (SYCE1 and CESC1) have been reported to localize exclusively to the CEs (Costa et al., 2005). In contrast to SYCP1, SYCP2 and -3 are structural components of AEs/LEs. Although SYCP2 bears limited homology with yeast Red1 over a short region, SYCP3 does not appear to have a yeast sequence homologue (Offenberg et al., 1998).

Recently, genes encoding the TF component SYCP1 and one of the AE components, SYCP3, have been disrupted in mice by gene targeting (Yuan et al., 2000; de Vries et al., 2005). In *Sycp1* mutant mice, normal AEs are formed; homologous chromosomes align with each other, but do not undergo synapsis (de Vries et al., 2005). Thus, the meiotic defects in the *Sycp1*-deficient mice reflect the functional implication of SYCP1 as a TF component. *Sycp3* knockout mice have been characterized in detail in several studies (Yuan et al., 2000, 2002; Pelttari et al., 2001; Kolas et al., 2004, 2005; Liebe et al., 2004; Kouznetsova et al., 2005). It was observed that, in $Sycp3^{-/-}$ spermatocytes, AEs are not formed and the other known AE component, SYCP2, fails to localize to axial chromosomal cores (Yuan et al., 2000; Pelttari et al., 2001). Thus, it was concluded that SYCP3 is a main determinant of AEs/LEs and that SYCP2 plays a role in shaping the in vivo structure of AEs/LEs (Pelttari et al., 2001).

Despite these extensive studies, the role of SYCP2 in the formation of AEs/LEs remains largely unknown, especially the question of whether SYCP2 is required for the incorporation of SYCP3 into AEs/LEs. To investigate the functions of SYCP2 in meiosis, we have cloned the full-length cDNA sequence for the mouse *Sycp2* gene. We report the generation of *Sycp2* mutant mice by gene targeting and the characterization of the essential role of SYCP2 in SC assembly and chromosomal synapsis in males. Our findings reveal novel insights into the molecular mechanisms underlying mammalian SC assembly. We demonstrate that SYCP2 is a primary determinant of AEs/LEs and is required for the incorporation of SYCP3 into the SC.

Results

Cloning of the mouse *Sycp2* gene

We previously identified *Sycp2* as a mouse germ cell–specific gene in our cDNA subtraction screen (Wang et al., 2001). We obtained the composite full-length *Sycp2* cDNA sequence (5 kb) by screening a testis cDNA library. The mouse SYCP2 protein (1,500 aa) shares 63 and 88% sequence identity with human and rat orthologues, respectively (Offenberg et al., 1998; Schalk et al., 1999). One striking feature of SYCP2 is the presence of a short coiled coil region near its COOH terminus (residues 1,379–1,433 in the mouse SYCP2), which is conserved in rat and human SYCP2 proteins. Antibodies were generated against the mouse SYCP2. Western blot analysis shows that SYCP2 migrates with an apparent molecular mass of 190 kD (Fig. 1 A). These antibodies were also characterized by the immunostaining of spread nuclei of spermatocytes and double immunostaining with a previously described anti-SYCP2 antibody to confirm that they are specific to SYCP2 (Fig. S1, available

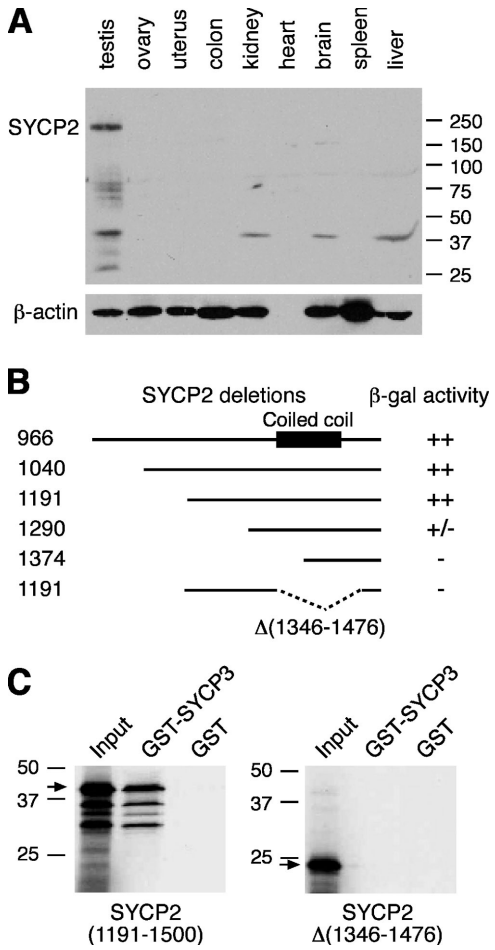

Figure 1. **Characterization of SYCP2 expression and its interaction with SYCP3.** (A) Western blot analysis of SYCP2 in adult mouse tissues. 30 μg of protein extracts were loaded. β-actin served as a loading control. Rabbit anti-SYCP2 polyclonal antibodies were used (1:500). (B) Identification of SYCP3-binding domain. Various truncated SYCP2 polypeptides were cloned in the pACT2 vector and tested for interaction with full-length mouse SYCP3 in the pAS2-1 vector by yeast two-hybrid β-galactosidase filter assay. ++, dark blue within 3 h of incubation; +/−, light blue within 5 h; −, not blue after overnight incubation. Numbers indicate the position of terminal residues in each clone. The coiled coil region is shown as a black box. (C) In vitro GST pulldown assay. Full-length SYCP3 protein (254 aa) was expressed as a GST fusion protein and affinity purified. The SYCP2 polypeptides (residues 1,191–1,500) with or without the deletion (residues 1,346–1,476) were translated in vitro and tested for binding with GST-SYCP3. Arrows indicate the in vitro–translated SYCP2 polypeptides. Molecular mass standards are shown in kilodaltons.

at http://www.jcb.org/cgi/content/full/jcb.200603063/DC1; Offenberg et al., 1998).

The coiled coil domain of SYCP2 is required for its binding to SYCP3

It has previously been established that SYCP2 interacts with SYCP3 in the yeast two-hybrid assay (Tarsounas et al., 1999). To define the SYCP3-binding domain, we generated NH_2-terminal truncations of SYCP2 and tested each of them for interaction with the full-length SYCP3. Our results show that the COOH-terminal 310-aa region of SYCP2 (residues 1,191–1,500) is necessary for its interaction with SYCP3 (Fig. 1 B). Additionally, the deletion of an internal region (residues 1,346–1,476) in SYCP2, including the coiled coil domain, abolishes its interaction with SYCP3 (Fig. 1 B). This interaction is further supported by results from in vitro GST pulldown experiments. Although the COOH-terminal SYCP2 polypeptide (residues 1,191–1,500) binds to GST-SYCP3, it fails to interact with GST-SYCP3 when the coiled coil–containing region (residues 1,346–1,476) is deleted (Fig. 1 C). Collectively, these data demonstrate that SYCP2 and -3 are able to form heterodimers or oligomers in vitro.

Disruption of the *Sycp2* gene

To elucidate the function of *Sycp2* in meiosis, we generated *Sycp2* mutant mice by homologous recombination in embryonic stem (ES) cells. The mouse *Sycp2* gene consists of 44 exons and spans a 70-kb genomic region. Exons 39–43 encode the SYCP2 region from residues 1,346–1,476, including the coiled coil domain, which is required for binding to SYCP3 (Fig. 1). In our targeting construct, the 1.9-kb genomic region harboring exons 39–43 is replaced with a floxed neomycin selection marker (Fig. 2 A). Therefore, deletion of the essential coiled coil domain is expected to disrupt the *Sycp2* gene.

To address whether the mutant *Sycp2* allele is transcribed, RT-PCR was performed on testis RNA from both wild-type and homozygous mutant ($Sycp2^{-/-}$) mice with primers residing within exons 38 and 44, respectively. As expected, the *Sycp2* mutant allele is, indeed, transcribed in testes (Fig. 2 B). Sequencing of the mutant RT-PCR product shows that splicing occurs from exons 38–44 without causing a frame shift. Furthermore, Western blot analysis demonstrates that the mutant SYCP2 protein without the coiled coil domain is produced in both $Sycp2^{+/-}$ and $Sycp2^{-/-}$ testes (Fig. 2 C). The truncated SYCP2 protein is referred to as SYCP2t.

SYCP2 is associated with SYCP3 in vivo

Our GST pulldown experiment shows that SYCP2 interacts with SYCP3 in vitro (Fig. 1 C). To address whether these two proteins are associated with each other in vivo, we performed coimmunoprecipitation experiments with soluble nuclear fractions of testicular protein extracts (Fig. 2 D). SYCP3 was completely immunoprecipitated with anti-SYCP3 antibody. In the wild type, SYCP2 immunoprecipitated with SYCP3. In contrast, SYCP2t was not coimmunoprecipitated, but rather stayed in the immunoprecipitated supernatant. Reciprocal immunoprecipitation experiments confirmed the association of SYCP2

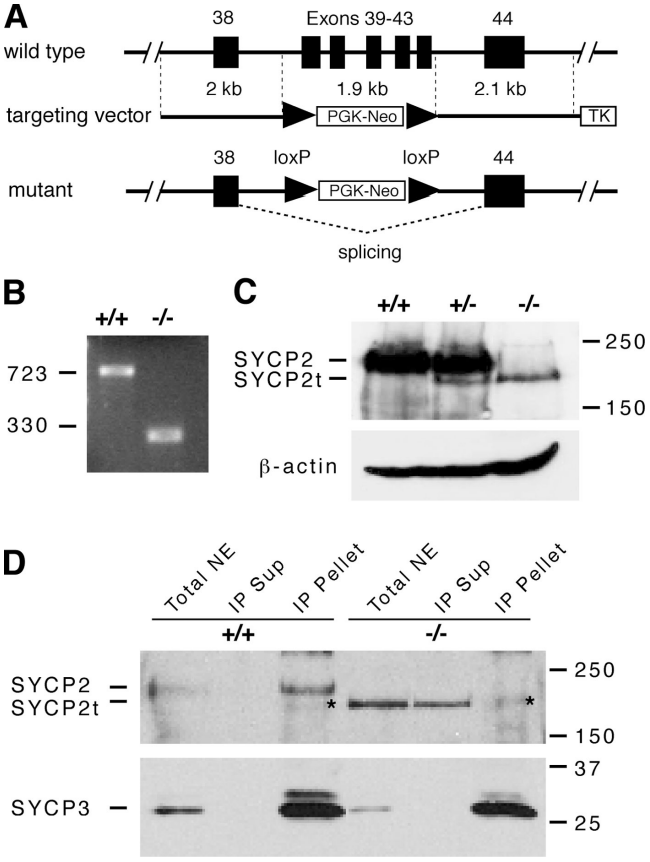

Figure 2. **Targeted disruption of the *Sycp2* gene.** (A) Schematic diagram of the *Sycp2* targeting strategy. Neomycin selection marker (PGK-Neo) was flanked by *loxP* sites. Thymidine kinase (TK) was included for negative selection with ganciclovir. Exons are shown in black boxes and designated by the numbers shown above the boxes. (B) Splicing of the mutant *Sycp2* transcript. RT-PCR was done with poly(A)$^+$ RNAs from wild-type (+/+) and *Sycp2* mutant (−/−) testes. PCR primers are located in exons 38 and 44. PCR product size is shown in bps. (C) Production of the mutant SYCP2t protein. Western blot analysis was performed on wild-type, $Sycp2^{+/-}$, and $Sycp2^{-/-}$ testicular protein extracts using rabbit anti-SYCP2 serum. (D) In vivo association of SYCP3 with SYCP2, but not SYCP2t. Soluble nuclear protein extracts from wild-type and $Sycp2^{-/-}$ testes were immunoprecipitated with anti-SYCP3 antibodies. Immunoblotting was probed with anti-SYCP2 antibodies. SYCP2, but not SYCP2t, was coimmunoprecipitated with SYCP3. *, a nonspecific diffuse band observed in the immunoprecipitated (IP) pellet of both wild-type and mutant. IP, immunoprecipitation; NE, nuclear extract; Sup, supernatant. Protein molecular mass standards are shown in kilodaltons.

and -3 (unpublished data). This set of experiments shows that SYCP2 is associated with SYCP3 in vivo and that the coiled coil region of SYCP2 is necessary for its binding to SYCP3.

Male sterility and meiotic arrest in *Sycp2*$^{-/-}$ mice

The $Sycp2^{-/-}$ mice appear to be healthy and normal in size. The fertility of $Sycp2^{-/-}$ mice is sexually dimorphic. The $Sycp2^{-/-}$ males are sterile, but $Sycp2^{-/-}$ females are subfertile. SYCP2t is expressed in $Sycp2^{+/-}$ testes (Fig. 2 C). However, both heterozygous ($Sycp2^{+/-}$) males and females are fertile, suggesting the absence of dominant-negative effects by SYCP2t. Interbreeding of $Sycp2^{+/-}$ mice yields a normal Mendelian ratio (27:78:35) of wild-type, $Sycp2^{+/-}$, and $Sycp2^{-/-}$ offspring.

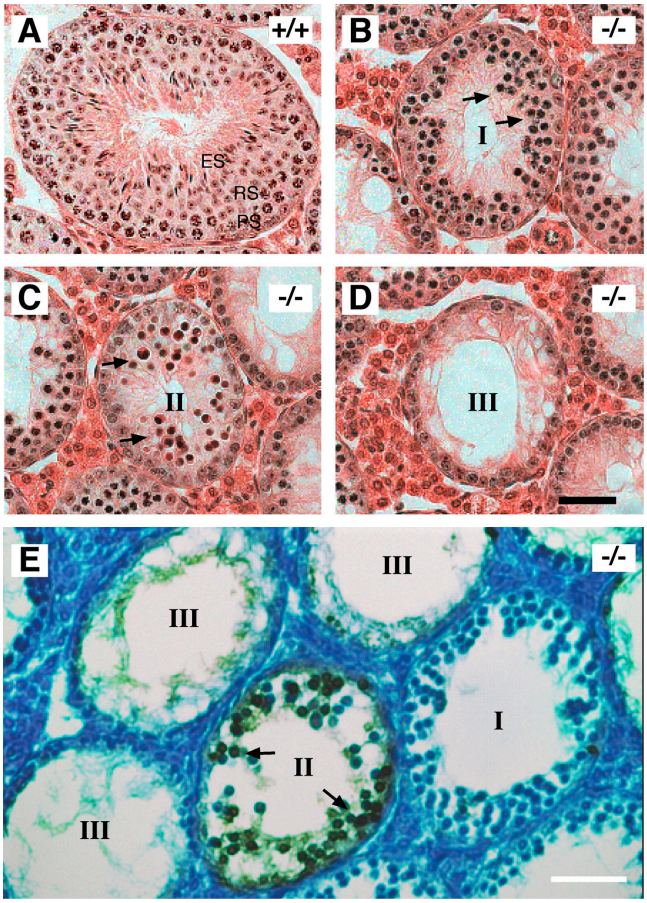

Figure 3. **Meiotic arrest and apoptosis of spermatocytes in *Sycp2*$^{-/-}$ mice.** Testes from 8-wk-old wild-type and *Sycp2*$^{-/-}$ mice were used for histological and apoptosis analyses. (A) Wild-type seminiferous tubule contains a full spectrum of germ cells: spermatogonia, pachytene spermatocytes (PS), round spermatids (RS), and elongated spermatids (ES). (B–D) Three types of tubules observed in *Sycp2*$^{-/-}$ testis. (B) In type I tubules, multiple layers of zygotene-like spermatocytes (arrows) are present. (C) In type II tubules, multiple layers of heavily eosin-stained cells (arrows) are present. (D) In type III tubules, only a single layer of spermatogonia and Sertoli cells are present. (E) Apoptosis of spermatocytes in type II *Sycp2*$^{-/-}$ tubules. Arrows indicate one or two layers of brown-stained apoptotic cells. Bars, 50 μm.

The weight of 8-wk-old *Sycp2*$^{-/-}$ testes is 70% less than that of the wild type. Seminiferous tubules in *Sycp2*$^{-/-}$ testes are significantly smaller in diameter than those in wild type (Fig. 3). Seminiferous tubules of wild-type testes contain a full spectrum of spermatogenic cells, including spermatogonia, spermatocytes, and spermatids (Fig. 3 A). In contrast, seminiferous tubules of *Sycp2*$^{-/-}$ testes exhibit complete meiotic arrest in spermatogenesis (Fig. 3, B–D). In *Sycp2*$^{-/-}$ testes, spermatogenic cells develop into zygotene-like spermatocytes, but fail to differentiate into normal pachytene spermatocytes (Fig. 3). Postmeiotic germ cells (round spermatids, elongating spermatids, and spermatozoa) are absent in *Sycp2*$^{-/-}$ seminiferous tubules. Three major types of seminiferous tubules are observed in *Sycp2*$^{-/-}$ testis. Type I tubules contain 2–3 layers of zygotene-like spermatocytes (Fig. 3 B). In type II tubules, zygotene-like spermatocytes are absent, but a few layers of heavily eosin-stained cells are present and might correspond to apoptotic cells (Fig. 3 C). Type III tubules are characterized by a single layer of spermatogonia/Sertoli cells (Fig. 3 D). Consistent with the histology of normal testes, epididymal tubules of the 8-wk-old wild-type mice are filled with spermatozoa, whereas those of the *Sycp2*$^{-/-}$ mice are empty (unpublished data). Collectively, these studies demonstrate that SYCP2 is required for meiosis and spermatogenesis in males.

Sycp2$^{-/-}$ spermatocytes undergo apoptosis

In type II tubules, germ cells are heavily eosin-stained, with increased chromatin density, suggesting that they undergo apoptosis (Fig. 3 C). A TUNEL assay shows the presence of many apoptotic cells in certain tubules, which are likely to correspond to type II tubules (Fig. 3 E). In contrast, no apoptotic cells are present in type I and III tubules (Fig. 3 E). Apoptosis of germ cells in type II tubules is also observed by electron microscopy (unpublished data). One possible explanation is that the presence of three types of tubules in *Sycp2*$^{-/-}$ testis might reflect coordinated differentiation of germ cells in a given tubule. The presence of three types of tubules could be explained as follows. In *Sycp2*$^{-/-}$ testis, spermatogenesis proceeds from spermatogonia, to the leptotene stage, to the zygotene stage, resulting in the accumulation of zygotene-like spermatocytes in type I tubules. Subsequently, these spermatocytes fail to differentiate into pachytene spermatocytes and undergo apoptosis in type II tubules. Eventually, all apoptotic spermatocytes are eliminated in type III tubules. No apoptotic cells are found in the epididymal tubules from *Sycp2*$^{-/-}$ mice, suggesting that apoptotic spermatocytes might be reabsorbed in the seminiferous tubules.

SYCP2 is required for chromosome synapsis in male meiosis

To determine the localization of SYCP1 and the extent of synapsis in *Sycp2*$^{-/-}$ spermatocytes, we performed immunostaining on spread spermatocytes with anti-SYCP1 antibodies and CREST antiserum (Kolas et al., 2005). In normal pachytene spermatocytes, homologous chromosomes are fully paired, and SYCP1 is localized to synapsed regions (Fig. 4 A). In *Sycp2*$^{-/-}$ testes, no pachytene spermatocytes are present, which is consistent with the histological analysis (Fig. 3). In *Sycp2*$^{-/-}$ spermatocytes, SYCP1 is present in several short fibers (Fig. 4 C), suggesting a failure in homologous chromosome synapsis.

CREST antiserum stains centromeres; therefore, it is used to determine the synaptic process in meiosis, along with DAPI staining of nuclei (Moens and Spyropoulos, 1995). During the leptotene stage, 40 centromeres (CREST foci) are expected. As synapsis proceeds, the number of CREST foci decreases. In pachytene spermatocytes, no more than 21 CREST foci are expected (Fig. 4, A and D; Scherthan et al., 1996). The number of CREST foci in zygotene spermatocytes ranges from 21 to 40. We analyzed >100 *Sycp2*$^{-/-}$ spermatocytes that showed positive SYCP1 staining. *Sycp2*$^{-/-}$ spermatocytes had 36 CREST foci/nucleus on average (36.0 ± 3.3; $n = 104$). No *Sycp2*$^{-/-}$ spermatocytes with >40 CREST foci were observed (Fig. 4, B and E), suggesting that sister chromatid cohesion at the centromeric regions is not affected. Interestingly, many CREST foci were present in pairs (Fig. 4, C and F).

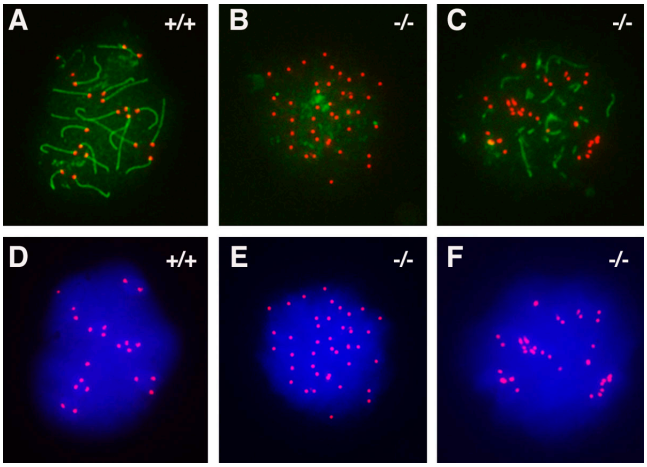

Figure 4. **Failure of chromosome synapsis in *Sycp2*$^{-/-}$ spermatocytes.** Spermatocytes from wild-type (A and D) and knockout (B, C, E, and F) mice were stained with anti-SYCP1 serum (green), CREST antiserum (red), and DAPI (blue). (A and D) In wild-type pachytene spermatocytes, SYCP1 labels SCs that have formed along synapsed homologous chromosomes. CREST antiserum marks 21 foci. (B and E) Early *Sycp2*$^{-/-}$ spermatocytes contain 40 CREST foci, suggesting that the cohesion of sister chromatids is not affected, at least not in the centromeric regions. SYCP1 is expressed, but apparently not in the form of fibers. (C and F) Many short SYCP1 fibers are present in advanced *Sycp2*$^{-/-}$ spermatocytes. There are ~34 CREST foci in this nucleus. Note that the CREST foci often exist in pairs.

SYCP2 is required for the incorporation of SYCP3 into AEs

To examine whether SYCP3 is localized to AEs/LEs in *Sycp2*$^{-/-}$ spermatocytes, we performed immunostaining with anti-SYCP3 antibodies and CREST antiserum. In wild-type pachytene spermatocytes, SYCP3 localizes to SCs (Fig. 5 A) and is present in *Sycp2*$^{-/-}$ testes, as determined by Western blotting (Fig. 2 D). Strikingly, in *Sycp2*$^{-/-}$ spermatocytes, SYCP3 accumulates as several large aggregates in the nucleus, but fails to localize to axial chromosome cores (Fig. 5 B, arrows). In addition, SYCP3 forms small nuclear foci (Fig. 5 B, arrowhead). Therefore, we conclude that SYCP2 is essential for the incorporation of SYCP3 into AEs/LEs.

SYCP2 is essential for formation of normal AEs

In *Sycp2*$^{-/-}$ spermatocytes, SYCP3 is not localized to axial chromosomal cores and, thus, is not suitable for analysis of AE formation (Fig. 5 B). It remains unclear whether AEs are still formed in *Sycp2*$^{-/-}$ spermatocytes. Silver nitrate stains AEs and paired LEs. Surface-spread nuclei of wild-type and *Sycp2*$^{-/-}$ spermatocytes are stained with silver nitrate (Dresser and Moses, 1979; Peters et al., 1997). Silver-stained SCs are abundant in wild type (Fig. 5 C). However, no silver-stained AEs are observed in *Sycp2*$^{-/-}$ spermatocytes after examining >100 spread nuclei (Fig. 5 D). Electron microscopy analysis of *Sycp2*$^{-/-}$ spermatocytes reveals the presence of CE-like structures with chromatins aligned to form SC-like structures (Fig. 5 F). However, these SC-like structures in *Sycp2*$^{-/-}$ spermatocytes lack typical LEs that are electron dense in wild-type spermatocytes (Fig. 5 E). Collectively, these observations are consistent with the lack of normal AEs in *Sycp2*$^{-/-}$ spermatocytes.

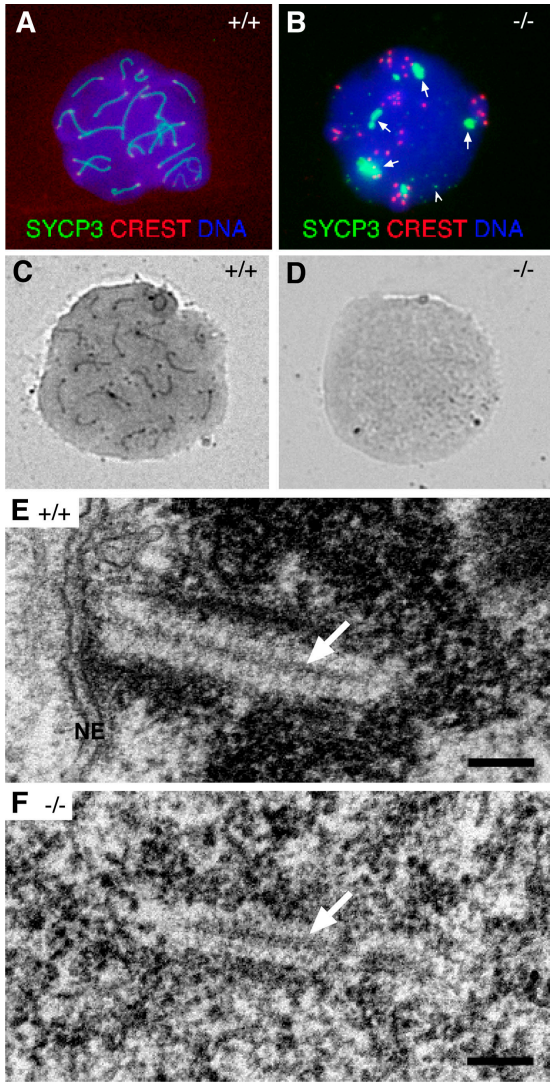

Figure 5. **Analysis of SC formation in *Sycp2*$^{-/-}$ spermatocytes.** Surface-spread nuclei were stained with anti-SYCP3 antibodies, CREST, and DAPI, or they were stained with silver nitrate. (A) SYCP3 labels SCs in wild-type spermatocytes. (B) SYCP3 fails to incorporate into SCs in *Sycp2*$^{-/-}$ spermatocytes. SYCP3 forms several large protein aggregates (arrows). In addition, SYCP3 also forms many small nuclear foci (arrowhead). (C) SCs in wild-type spermatocytes are readily stained with silver nitrate. (D) No silver-stained SC structures are visible by light microscopy in *Sycp2*$^{-/-}$ spermatocytes. (E) EM analysis of a wild-type spermatocyte. A tripartite structure of SC is formed by one CE (arrow) that connects with two electron-dense LEs. This SC is attached to the nuclear envelope (NE). Note the condensed chromatin around the SC. (F) EM analysis of a *Sycp2*$^{-/-}$ spermatocyte. TFs form a CE-like structure (arrow). Two rows of chromatin grains align in parallel with the CE-like structure to form a SC-like structure. Bars, 0.2 μm.

Cohesin complexes connect sister chromatids during mitosis and meiosis (Page and Hawley, 2004). Cohesin proteins are required for assembly of AEs/LEs in diverse organisms. STAG3 is a mammalian meiosis-specific cohesin (Prieto et al., 2001). STAG3 apparently localizes to axial chromosomal cores (cohesin complexes) in wild-type spermatocytes (Fig. S2, available at http://www.jcb.org/cgi/content/full/jcb.200603063/DC1). In *Sycp2*$^{-/-}$ spermatocytes, STAG3 still localizes to long fibers (Fig. 6, H and I; and Fig. S2), which correspond to

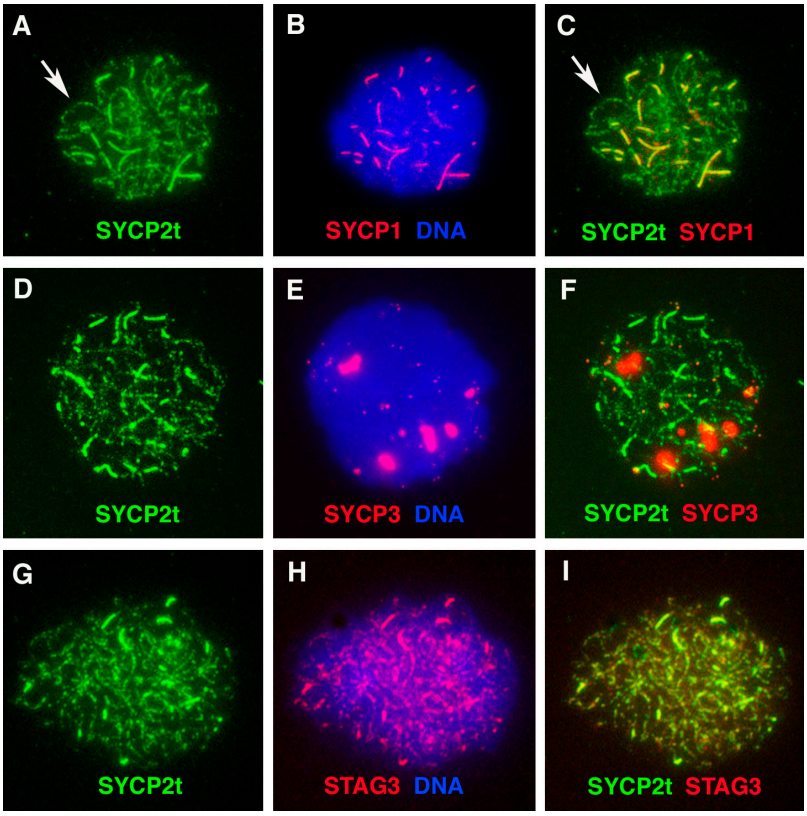

Figure 6. **Association of SYCP2t with axial chromosomal cores in *Sycp2*$^{-/-}$ spermatocytes.** Surface-spread nuclei of *Sycp2*$^{-/-}$ spermatocytes were immunostained with guinea pig anti-SYCP2 serum and anti-SYCP1, or anti-SYCP3, or anti-STAG3 antibodies. DNA was stained with DAPI. Arrows (A and C) indicate a fine fiber with a bead-on-a-string appearance. The three images in each row represent the same *Sycp2*$^{-/-}$ spermatocyte.

cohesin complexes formed along common cores of sister chromatids, suggesting that SYCP2 is not required for sister chromatid cohesion.

SYCP2t localizes to axial chromosomal cores

The SYCP2t protein is made in the *Sycp2*$^{-/-}$ spermatocytes (Fig. 2 C). To address whether SYCP2t is able to associate with axial chromosomal cores, we performed immunofluorescence on *Sycp2*$^{-/-}$-spread nuclei (Fig. 6). First, SYCP2t colocalizes to thick fibers with SYCP1, which are continuous, but variable in length (Fig. 6 C). Second, SYCP2t is observed in fine fibers, where SYCP1 is absent. Close examination reveals that these fine fibers are not uniform in staining and appear as bead-on-a-string arrays (Fig. 6, A–C). This staining is likely to reflect authentic SYCP2t localization rather than nonspecific background because it is observed with polyclonal antibodies from two rabbits and two guinea pigs. In addition, the same localization pattern is obtained using antibodies raised against a different region of SYCP2 (Fig. S3, available at http://www.jcb.org/cgi/content/full/jcb.200603063/DC1; Offenberg et al., 1998). As expected, SYCP3 does not colocalize with SYCP2t in the *Sycp2*$^{-/-}$ spermatocytes (Fig. 6 F). Furthermore, SYCP2t colocalizes with STAG3 in both thick and fine fibers in *Sycp2*$^{-/-}$ spermatocytes (Fig. 6), suggesting that SYCP2t is associated with axial chromosomal cores.

We next examined the association of SC proteins with chromatin using different fractions of testicular extracts: cytoplasmic, nuclear, and chromatin (Fig. 7). During the preparation of nuclear extracts, nuclear proteins are bound to the chromatin pellet in various degrees. As expected, the core histones, such as histone H3, are tightly bound to chromatin. Although the majority of SYCP1 is present in the nuclear extract, a significant amount is associated with chromatin in both wild-type and *Sycp2*$^{-/-}$ testes. In contrast, SYCP2 and -3 behave differently. In wild-type, most SYCP2 is tightly bound to chromatin (Fig. 7, lane 4). Although SYCP2t localizes to axial chromosomal cores, the majority of SYCP2t can be extracted from chromatin (Fig. 7, lane 7), suggesting that its association with chromatin is significantly weakened by the deletion of the coiled coil domain. Slightly less than half of SYCP3 in the wild-type testes, but virtually none of SYCP3 in the *Sycp2*$^{-/-}$ testes, is associated with chromatin (Fig. 7), which is consistent with the immunolocalization data (Fig. 6 F).

Reduced female fertility in *Sycp2*$^{-/-}$ mice

To characterize the function of SYCP2 in female germ cells, 8-wk-old *Sycp2*$^{-/-}$ females and wild-type littermates (10 mice/genotype) were mated with wild-type males for 2 mo. The mice were checked daily, and the number of offspring was recorded. In contrast to the sterility of *Sycp2*$^{-/-}$ males, *Sycp2*$^{-/-}$ females produced viable offspring. However, *Sycp2*$^{-/-}$ females displayed a dramatic decrease in litter size, producing on average 4.4 offspring per litter (4.4 ± 1.5; $n = 16$ litters). In comparison, wild-type littermates generated 7.8 offspring per litter (7.8 ± 1.7; $n = 16$ litters; $P < 0.0001$).

Histological analysis of adult *Sycp2*$^{-/-}$ ovaries revealed no apparent defects in follicular development (unpublished data). However, we examined surface-spread fetal oocytes that were obtained from *Sycp2*$^{-/-}$ females at 17.5 d postcoitum (dpc)

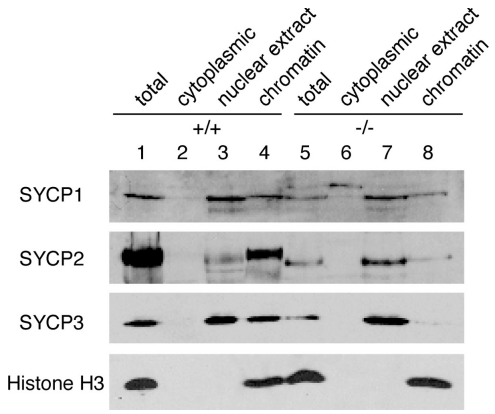

Figure 7. **Association of SC proteins with chromatin.** Cytoplasmic, nuclear, and chromatin extracts were sequentially prepared from wild-type and *Sycp2*$^{-/-}$ testes. Equal fractions of nuclear and chromatin extracts were loaded. The same preparations were subjected to Western blot analysis with antibodies against SYCP1, -2, -3, and histone H3. Histone H3 is a core histone and, thus, is tightly bound to chromatin.

and found that although mutant oocytes exhibit homologous chromosome alignments, as determined by SYCP1 staining, full chromosome synapsis is interrupted by the presence of prominent axial gaps in the SC (Fig. 8 A). Moreover, whereas SYCP2t localizes to axial chromosomal cores, SYCP3 failed to do so in *Sycp2*$^{-/-}$ oocytes (Fig. 8 B). In these oocytes, SYCP3 was found in several large nuclear aggregates (Fig. 8 B, arrows). Interestingly, remnant SYCP3 staining was also detected as prominent nuclear foci that were consistently associated with chromosome ends at the pachytene stage of meiosis (Fig. 8 B, arrowheads). Moreover, a detailed analysis of the distribution of SYCP3 protein in *Sycp2*$^{-/-}$ oocytes revealed that about half of the SYCP3 foci are associated with CREST signals (unpublished data). These findings are consistent with a possible association of SYCP3 protein with telomeric regions of pachytene stage chromosomes in *Sycp2*$^{-/-}$ oocytes. Double immunostaining analysis with anti-SYCP1 antibody and CREST antiserum revealed that centromere pairing occurs in the majority of *Sycp2*$^{-/-}$ oocytes, which is consistent with the formation of homologous chromosome synapsis (Fig. 9).

Discussion

SYCP2 is known as a structural component of the AEs/LEs of mammalian SCs. Gene targeting studies of the *Sycp2* locus have not been reported. In this study, we generated *Sycp2* mutant mice by deleting a coiled coil region required for binding to SYCP3. The phenotype of *Sycp2* mutant mice is sexually dimorphic; males are sterile because of the absence of AE formation and the subsequent disruption of chromosome synapsis in prophase I spermatocytes, and females are subfertile. These phenotypes have also been observed in *Sycp3*-deficient mice (Yuan et al., 2000, 2002; Pelttari et al., 2001; Kolas et al., 2004, 2005; Liebe et al., 2004; Kouznetsova et al., 2005). However, our studies with

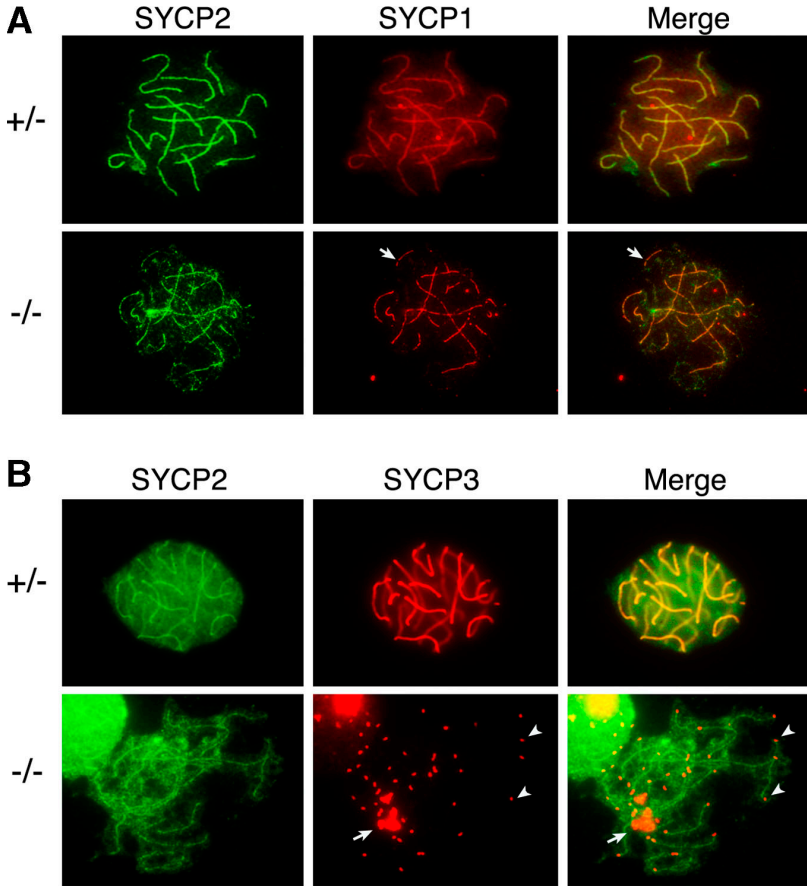

Figure 8. **Localization of SYCP1, 2 and 3 in *Sycp2*$^{-/-}$ oocytes.** Oocytes from embryonic ovaries at 17.5 dpc were analyzed by immunostaining. *Sycp2*$^{+/-}$ littermates were used as controls. (A) SYCP1 and -2 localize to fully synapsed and continuous SCs in a *Sycp2*$^{+/-}$ pachytene oocyte. However, axial gaps and interrupted synapsis are prominent in *Sycp2*$^{-/-}$ oocytes, as indicated by arrows (this oocyte is at the late pachytene/early diplotene stage). (B) Localization of SYCP3 in *Sycp2*$^{-/-}$ oocytes. SYCP3 fails to localize to AEs, but instead forms a few large nuclear aggregates (arrow). In addition, many small SYCP3 foci are present at chromosome ends (arrowheads).

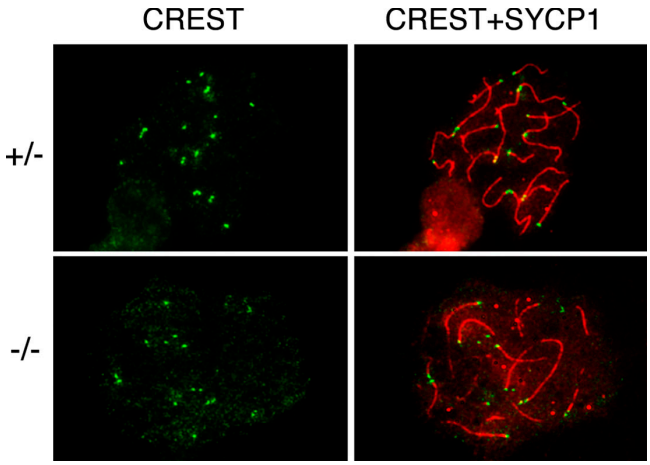

Figure 9. **Pairing of homologous chromosomes in *Sycp2*$^{-/-}$ oocytes.** *Sycp2*$^{+/-}$ and *Sycp2*$^{-/-}$ oocytes at 17.5 dpc were stained with CREST antiserum (green) and anti-SYCP1 antibodies (red). Control pachytene stage oocyte exhibited 20 CREST foci (centromeres) and full synapsis of homologous chromosomes (top). Chromosome pairing was present in *Sycp2*$^{-/-}$ oocytes (bottom).

Sycp2 mutant mice reveal novel insights into the mechanism of assembly of AEs/LEs in mammalian spermatogenesis.

SYCP2 and -3 form heterodimers or oligomers

SYCP3, but not SYCP2, is able to form multistranded fibers when ectopically expressed in cultured cells (Yuan et al., 1998; Pelttari et al., 2001). SYCP3 interacts with itself in a yeast two-hybrid assay (Tarsounas et al., 1997). These studies suggest that SYCP3 is capable of forming homooligomers. Several lines of evidence support that SYCP2 and -3 interact with each other. First, ultrastructural studies have shown that both SYCP2 and -3 localize to the AEs/LEs (Offenberg et al., 1998; Schalk et al., 1998). Second, SYCP2 and -3 form novel fibers when coexpressed in COS cells (Pelttari et al., 2001). Third, SYCP2 interacts with SYCP3 in yeast two-hybrid assay (Tarsounas et al., 1999), which is confirmed in this study (Fig. 1 B). We demonstrate that the evolutionarily conserved coiled coil domain in SYCP2 is essential for binding to SYCP3. Fourth, SYCP2 and -3 interact with each other in GST pulldown experiments (Fig. 1 C). Finally, our coimmunoprecipitation experiments show that SYCP2 and -3 are associated with each other in vivo (Fig. 2 D). Importantly, deletion of the coiled coil–containing region of SYCP2 abolishes SYCP2–SYCP3 interaction in yeast two-hybrid, GST pulldown, and coimmunoprecipitation assays, as well as colocalization studies. Collectively, we conclude that SYCP2 and -3 exist as heterodimers/oligomers in SCs.

SYCP2 is a primary determinant of mammalian AEs/LEs

SYCP2 is required for the incorporation of SYCP3 into AEs/LEs. In *Sycp2*$^{-/-}$ spermatocytes and fetal oocytes, SYCP3 accumulates as large protein aggregates in the nuclei, but fails to bind axial chromosomal cores (Fig. 5 B and Fig. 8 B). Aggregation of SYCP3 in *Sycp2* mutant spermatocytes is expected because SYCP3 forms multistranded fibers when ectopically expressed in cultured cells (Yuan et al., 1998). In contrast with the aggregation of SYCP3 in *Sycp2*$^{-/-}$ spermatocytes and oocytes, SYCP2t is still associated with axial chromosomal cores, suggesting that SYCP2t binds to axial chromosomal cores through proteins other than SYCP3. Our data support the hypothesis that SYCP2 is a primary determinant of mammalian AEs/LEs and that SYCP3 becomes incorporated into AEs/LEs via SYCP2. Thus, the expression of SYCP2t in the mutant testis is informative in dissecting two distinct SYCP2 functions, association with axial chromosomal cores, and binding to SYCP3. Our results demonstrate that these two SYCP2 functions are genetically separable.

In *Sycp3*-deficient spermatocytes and oocytes, SYCP2 fails to assemble along the axial chromosomal cores, leading to the hypothesis that SYCP3 is a main determinant of AEs/LEs (Pelttari et al., 2001; Yuan et al., 2002). It is puzzling that wild-type SYCP2 fails to localize to axial chromosomal cores in the absence of SYCP3. It is not apparent why the localization of SYCP2 in *Sycp3*$^{-/-}$ germ cells is different from that of SYCP2t in *Sycp2*$^{-/-}$ germ cells. We postulate two possibilities. First, other than being a structural protein, SYCP3 might play an unknown regulatory role in the association of SYCP2 with axial chromosomal cores. Therefore, in the absence of SYCP3, SYCP2 is not able to associate with axial chromosomal cores, which is the case in *Sycp3*-deficient spermatocytes and oocytes (Pelttari et al., 2001; Yuan et al., 2002). However, in *Sycp2*$^{-/-}$ spermatocytes and oocytes, the regulatory role of SYCP3 is intact and, thus, allows SYCP2t to associate with axial chromosomal cores (Figs. 6 and 8). A second possibility is that the SYCP2t protein gains a new, but artificial, axial chromosomal core–binding function. A double *Sycp2 Sycp3* mouse mutant will be informative in testing these two possibilities.

Mammalian genetics of SYCPs and sexual dimorphism of fertility

SYCP1, -2, and -3 are known structural components of SCs in mammals (Heyting et al., 1989). To date, all three encoding genes have been disrupted in mice (Yuan et al., 2000; de Vries et al., 2005; this study). Studies of these mutant mice have provided invaluable insights into SC assembly, chromosome synapsis, and fertility. As expected based on a previous study (Heyting et al., 1989), these genetic mutants corroborate previous conclusions and predictions. As a component of TFs, SYCP1 is required for chromosomal synapsis, but not for AE assembly and homologous chromosomal pairing (de Vries et al., 2005). As components of AEs/LEs, both SYCP2 and -3 are required for formation of AEs and chromosome synapsis in males. However, these genetic studies have also provided unexpected new insights. For instance, SYCP1 is required for the formation of the XY body in pachytene spermatocytes (de Vries et al., 2005). In *Sycp2* or *-3* mutant spermatocytes, SYCP1 still forms short fibers in the absence of AEs/LEs, suggesting that SYCP1 binds directly to chromatin or interacts with other chromatin structures, such as sister chromatid cohesion complexes (Pelttari et al., 2001). Our studies of a unique *Sycp2* mouse mutant demonstrate that SYCP2 is a primary determinant of AEs/LEs.

Although disruption of *Sycp1* affects the fertility of both sexes, the fertility of *Sycp2* and *-3* mutant mice is sexually dimorphic; males are sterile, but females are subfertile (Yuan et al., 2000, 2002; de Vries et al., 2005; this study). Both *Sycp2* and *-3* mutant spermatocytes are arrested at the zygotene stage of meiotic prophase I and exhibit failure in chromosomal synapsis. SYCP1 only forms short fibers in *Sycp2* or *-3* mutant spermatocytes. In contrast, both *Sycp2* and *-3* mutant oocytes exhibit a type of chromosome synapsis, in which SYCP1 localizes to long fibers that are interrupted by some axial gaps. Therefore, both *Sycp2* and *-3* mutant females are fertile, but with reduced litter size. Furthermore, *Sycp3* mutant females exhibit increased aneuploidy in oocytes and in embryo death (Yuan et al., 2002).

Strikingly, a growing number of meiosis-defective mouse mutants display sexual dimorphism of fertility (Hunt and Hassold, 2002; Kolas et al., 2005). One possible explanation for sexual dimorphism of fertility is that the control mechanisms of meiosis are more stringent in males (Hunt and Hassold, 2002). Even though the meiotic prophase of males and females is similar in many aspects, such as synapsis and homologous recombination, there are several notable kinetic and developmental differences (Hunt and Hassold, 2002; Kolas et al., 2005). In mouse, females initiate meiosis at embryonic day 13.5. Males do not initiate meiosis until puberty. In females, the progression of meiotic prophase is largely a one-time embryonic event, whereas spermatocyte development in adult testis is continuous and nonsynchronous. Another prominent difference is the behavior of the sex chromosomes. The XY chromosomes are sequestered in the XY bodies in pachytene spermatocytes and form synapsis only in the pseudoautosomal regions. In contrast, the XX chromosomes are synapsed along their entire length and undergo homologous recombination in oocytes. A recent study of meiotic mouse mutants (*Sycp3*, *Brca1*, and *Fkbp6*) further supports the hypothesis that sexual dimorphism of fertility reflects different developmental pathways underlying the meiotic prophase in males and females (Kolas et al., 2005).

Materials and methods

Cloning of the full-length *Sycp2* cDNA sequence
A lambda phage cDNA library was screened essentially as previously described (Wang and Page, 2002). In brief, lambda phage lysates were prepared from 24 subpools (~80,000 clones each) of the mouse testis cDNA library (BD Biosciences) and used as PCR templates. *Sycp2*-positive subpools were identified by PCR with *Sycp2*-specific primers chosen from previously obtained partial *Sycp2* sequences (Wang et al., 2001). 5′ and 3′ cDNA fragments were amplified separately from positive subpools by PCR, in which one *Sycp2*-specific primer and one vector primer were used. PCR products were sequenced. The composite *Sycp2* cDNA sequence has been deposited in GenBank under accession no. DQ103262.

Generation of anti-SYCP2 polyclonal antibodies
The *Sycp2* cDNA fragment corresponding to residues 1,255–1,500 was cloned into the pQE-30 vector (QIAGEN). The 6× His-SYCP2 fusion protein was expressed in M15 bacteria, purified with Ni-NTA resin, and eluted in 8 M urea. Two rabbits and two guinea pigs were immunized with the recombinant SYCP2 protein (Cocalico Biologicals, Inc.). The anti-SYCP2 antiserum (serum 1918 and GP21) was used for Western blot (1:500) and immunofluorescence (1:100).

Yeast two-hybrid and in vitro GST pulldown assays
Various truncated *Sycp2* fragments were cloned in the pACT2 vector (BD Biosciences). Mouse *Sycp3* coding region was amplified from bulk testis cDNAs by PCR, cloned into the pAS2-1 vector (BD Biosciences), and sequenced. Interaction between SYCP3 and various SYCP2 proteins were assayed by cotransformation into the reporter yeast strain Y190, followed by standard β-galactosidase filter assay. Full-length SYCP3 was cloned into pGEX4T-1, expressed as a GST fusion protein in bacteria, and affinity purified. SYCP2 fragments were produced in the presence of [^{35}S]methionine using the TNT in vitro transcription and translation kit (Promega). GST pulldown assays were performed as previously described (May et al., 2002).

Targeted disruption of the *Sycp2* Gene
In the targeting construct, the 1.9-kb genomic DNA harboring exons 39–43 was replaced with a floxed neomycin selection cassette (Fig. 2 A). The two homologous arms (2 and 2.1 kb) were amplified by PCR with high-fidelity DNA polymerase from a *Sycp2*-containing bacterial artificial chromosome clone (RP23-160K5). The thymidine kinase–negative selection marker was cloned adjacent to the right arm. The V6.5 ES cells were electroporated with the linearized targeting construct and were cultured in the presence of 350 μg/ml G418 and 2 μM ganciclovir. 48 double-resistant ES cell clones were recovered and screened for homologous recombination events by long-distance PCR. Five clones were produced by homologous recombination via both arms. Two clones (A4 and C6) were injected into B6C3F1 blastocysts (Taconic). No difference in phenotypes was observed between mice derived from these two ES clones. All of the studies were performed with mice from clone C6. All of the offspring were genotyped by PCR. The wild-type allele was assayed by PCR (400 bp) with the primers AGATGAGGGCATATCACCGA and TAAGCACACTCACCATCTCC. The PCR product (300 bp) of the mutant allele was amplified by PCR with the primers GCATGTTATCAACCTTATCCCT and CCTACCGGTGGATGTGGAATGTGTG. RT-PCR for splicing assays was performed with the following primers, which were located in exons 38 and 44: TCTGTTCCTAAGGACTGGCA and TACAAGCTGCATTTGGAGTCA. All of the experiments involving mice were approved by the Institutional Animal Care and Use Committee at the University of Pennsylvania.

TUNEL assay
Testes from wild-type and *Sycp2*$^{-/-}$ mice were fixed in 10% (vol/vol) neutral buffered formalin (Fisher Scientific) and embedded in paraffin. 8-μm-thick testis sections were cut and used for TUNEL assay. TUNEL assays were performed with the ApopTag peroxidase in situ Apoptosis Detection kit according to the manufacturer's instructions (CHEMICON International, Inc.). Samples were counterstained briefly in 0.5% (wt/vol) methyl green and visualized on a microscope (Axioskop 40; Carl Zeiss MicroImaging, Inc.).

Histology, surface nuclei spread, and immunofluorescence
For histology, testes were fixed in Bouin's solution, embedded in paraffin, sectioned, and stained with hematoxylin and eosin. Surface spread of spermatocyte nuclei was performed as previously described (Peters et al., 1997; Kolas et al., 2005). To obtain fetal oocytes, *Sycp2*$^{-/-}$ females were mated with *Sycp2*$^{+/-}$ males. Vaginal copulatory plugs were checked the next morning. Fetal oocytes were collected for analysis at 17.5 dpc. The primary antibodies used for immunofluorescence were as follows: anti-SYCP1 (a gift from P. Moens and B. Spyropoulos [York University, Toronto, Ontario, Canada] and C. Höög [Karolinska Institute, Stockholm, Sweden]; Dobson et al., 1994; Liu et al., 1996; Schmekel et al., 1996), anti-SYCP2 serum 493 (1:400; a gift from C. Heyting, Wageningen University, Wageningen, Netherlands; Offenberg et al., 1998), anti-SYCP3 (1:500; a gift from S. Chuma, Kyoto University, Kyoto, Japan; Chuma and Nakatsuji, 2001), anti-STAG3 (1:500; a gift from J.L. Barbero, Centro Nacional de Biotecnologia, Madrid, Spain; Prieto et al., 2001), FITC-conjugated anti-γH2AX (1:500; Upstate Biotechnology), and CREST antiserum (1:5,000; a gift from B.R. Brinkley, Baylor College of Medicine, Houston, TX). Tissue sections were visualized under an Axioskop 40 microscope. Images were captured with a digital camera (Evolution QEi; MediaCybernetics) and processed with ImagePro software (Phase 3 Imaging Systems) and Photoshop (Adobe).

EM
EM was performed at the Biomedical Imaging Core facility at the University of Pennsylvania, as previously described (Yang et al., 1997). In brief, 21-d-old testes were fixed in 2.5% glutaraldehyde and 2% paraformaldehyde

for 4 h, and then postfixed in 1% osmium tetroxide for 1 h. The specimens were dehydrated in ethanol, transferred to propylene oxide, and embedded in EM-Bed 812 medium (Electron Microscopy Sciences). The specimens were polymerized at 68°C for 48 h. Ultrathin sections were cut with a diamond knife, mounted on single-hole grids, stained with bismuth solution, and examined with an electron microscope (Tecnai-T12; FEI). Digital images were captured with a charge-coupled device camera (Gatan, Inc.).

Online supplemental material

Fig. S1 shows the immunostaining of SCs with our anti-SYCP2 serum to demonstrate the specificity of this antibody. Fig. S2 shows the distribution of STAG3 and γH2AX in wild-type and *Sycp2*$^{-/-}$ spermatocytes. Fig. S3 shows localization of SYCP2t to axial chromosomal cores in *Sycp2*$^{-/-}$ spermatocytes with two different anti-SYCP2 antibodies (Offenberg et al., 1998). Online supplemental material is available at http://www.jcb.org/cgi/content/full/jcb.200603063/DC1.

We thank E. Gleason for technical assistance, Q.C. Yu for EM, P. Moens and B. Spyropoulos for anti-SYCP1 antibodies and spread protocols, C. Höög for anti-SYCP1, C. Heyting for anti-SYCP2, J.L. Barbero for anti-STAG3, S. Chuma for anti-SYCP3 antibodies, B.R. Brinkley for CREST, and J.R. Pehrson for scientific discussions. We thank N.G. Avadhani and R. Schultz for comments on the manuscript.

This work was supported by start-up funds from the University of Pennsylvania and the Commonwealth and General Assembly of Pennsylvania to P.J. Wang. R. De La Fuente is supported by grant HD042740 from the National Institutes of Health.

Submitted: 14 March 2006
Accepted: 18 April 2006

References

Bailis, J.M., and G.S. Roeder. 1998. Synaptonemal complex morphogenesis and sister-chromatid cohesion require Mek1-dependent phosphorylation of a meiotic chromosomal protein. *Genes Dev.* 12:3551–3563.

Chuma, S., and N. Nakatsuji. 2001. Autonomous transition into meiosis of mouse fetal germ cells in vitro and its inhibition by gp130-mediated signaling. *Dev. Biol.* 229:468–479.

Colaiacovo, M.P., A.J. MacQueen, E. Martinez-Perez, K. McDonald, A. Adamo, A. La Volpe, and A.M. Villeneuve. 2003. Synaptonemal complex assembly in *C. elegans* is dispensable for loading strand-exchange proteins but critical for proper completion of recombination. *Dev. Cell*. 5:463–474.

Costa, Y., R. Speed, R. Ollinger, M. Alsheimer, C.A. Semple, P. Gautier, K. Maratou, I. Novak, C. Hoog, R. Benavente, and H.J. Cooke. 2005. Two novel proteins recruited by synaptonemal complex protein 1 (SYCP1) are at the centre of meiosis. *J. Cell Sci.* 118:2755–2762.

de los Santos, T., and N.M. Hollingsworth. 1999. Red1p, a MEK1-dependent phosphoprotein that physically interacts with Hop1p during meiosis in yeast. *J. Biol. Chem.* 274:1783–1790.

de Vries, F.A., E. de Boer, M. van den Bosch, W.M. Baarends, M. Ooms, L. Yuan, J.G. Liu, A.A. van Zeeland, C. Heyting, and A. Pastink. 2005. Mouse *Sycp1* functions in synaptonemal complex assembly, meiotic recombination, and XY body formation. *Genes Dev.* 19:1376–1389.

Dobson, M.J., R.E. Pearlman, A. Karaiskakis, B. Spyropoulos, and P.B. Moens. 1994. Synaptonemal complex proteins: occurrence, epitope mapping and chromosome disjunction. *J. Cell Sci.* 107:2749–2760.

Dresser, M.E., and M.J. Moses. 1979. Silver staining of synaptonemal complexes in surface spreads for light and electron microscopy. *Exp. Cell Res.* 121:416–419.

Fawcett, D.W. 1956. The fine structure of chromosomes in the meiotic prophase of vertebrate spermatocytes. *J. Biophys. Biochem. Cytol.* 2:403–406.

Friedman, D.B., N.M. Hollingsworth, and B. Byers. 1994. Insertional mutations in the yeast HOP1 gene: evidence for multimeric assembly in meiosis. *Genetics*. 136:449–464.

Heyting, C., A.J. Dietrich, P.B. Moens, R.J. Dettmers, H.H. Offenberg, E.J. Redeker, and A.C. Vink. 1989. Synaptonemal complex proteins. *Genome*. 31:81–87.

Hollingsworth, N.M., and L. Ponte. 1997. Genetic interactions between HOP1, RED1 and MEK1 suggest that MEK1 regulates assembly of axial element components during meiosis in the yeast *Saccharomyces cerevisiae*. *Genetics*. 147:33–42.

Hunt, P.A., and T.J. Hassold. 2002. Sex matters in meiosis. *Science*. 296:2181–2183.

Kolas, N.K., L. Yuan, C. Hoog, H.H. Heng, E. Marcon, and P.B. Moens. 2004. Male mouse meiotic chromosome cores deficient in structural proteins SYCP3 and SYCP2 align by homology but fail to synapse and have possible impaired specificity of chromatin loop attachment. *Cytogenet. Genome Res.* 105:182–188.

Kolas, N.K., E. Marcon, M.A. Crackower, C. Hoog, J.M. Penninger, B. Spyropoulos, and P.B. Moens. 2005. Mutant meiotic chromosome core components in mice can cause apparent sexual dimorphic endpoints at prophase or X-Y defective male-specific sterility. *Chromosoma*. 114:92–102.

Kouznetsova, A., I. Novak, R. Jessberger, and C. Hoog. 2005. SYCP2 and SYCP3 are required for cohesin core integrity at diplotene but not for centromere cohesion at the first meiotic division. *J. Cell Sci.* 118:2271–2278.

Lammers, J.H., H.H. Offenberg, M. van Aalderen, A.C. Vink, A.J. Dietrich, and C. Heyting. 1994. The gene encoding a major component of the lateral elements of synaptonemal complexes of the rat is related to X-linked lymphocyte-regulated genes. *Mol. Cell. Biol.* 14:1137–1146.

Liebe, B., M. Alsheimer, C. Hoog, R. Benavente, and H. Scherthan. 2004. Telomere attachment, meiotic chromosome condensation, pairing, and bouquet stage duration are modified in spermatocytes lacking axial elements. *Mol. Biol. Cell*. 15:827–837.

Liu, J.G., L. Yuan, E. Brundell, B. Bjorkroth, B. Daneholt, and C. Hoog. 1996. Localization of the N-terminus of SCP1 to the central element of the synaptonemal complex and evidence for direct interactions between the N-termini of SCP1 molecules organized head-to-head. *Exp. Cell Res.* 226:11–19.

MacQueen, A.J., M.P. Colaiacovo, K. McDonald, and A.M. Villeneuve. 2002. Synapsis-dependent and -independent mechanisms stabilize homolog pairing during meiotic prophase in *C. elegans*. *Genes Dev.* 16:2428–2442.

May, M.J., R.B. Marienfeld, and S. Ghosh. 2002. Characterization of the IκB-kinase NEMO binding domain. *J. Biol. Chem.* 277:45992–46000.

Meuwissen, R.L., H.H. Offenberg, A.J. Dietrich, A. Riesewijk, M. van Iersel, and C. Heyting. 1992. A coiled-coil related protein specific for synapsed regions of meiotic prophase chromosomes. *EMBO J.* 11:5091–5100.

Moens, P.B., and B. Spyropoulos. 1995. Immunocytology of chiasmata and chromosomal disjunction at mouse meiosis. *Chromosoma*. 104:175–182.

Moses, M.J. 1956. Chromosomal structures in crayfish spermatocytes. *J. Biophys. Biochem. Cytol.* 2:215–218.

Moses, M.J. 1969. Structure and function of the synaptonemal complex. *Genetics*. 61:41–51.

Offenberg, H.H., J.A. Schalk, R.L. Meuwissen, M. van Aalderen, H.A. Kester, A.J. Dietrich, and C. Heyting. 1998. SCP2: a major protein component of the axial elements of synaptonemal complexes of the rat. *Nucleic Acids Res.* 26:2572–2579.

Page, S.L., and R.S. Hawley. 2001. *c(3)G* encodes a *Drosophila* synaptonemal complex protein. *Genes Dev.* 15:3130–3143.

Page, S.L., and R.S. Hawley. 2004. The genetics and molecular biology of the synaptonemal complex. *Annu. Rev. Cell Dev. Biol.* 20:525–558.

Pelttari, J., M.R. Hoja, L. Yuan, J.G. Liu, E. Brundell, P. Moens, S. Santucci-Darmanin, R. Jessberger, J.L. Barbero, C. Heyting, and C. Hoog. 2001. A meiotic chromosomal core consisting of cohesin complex proteins recruits DNA recombination proteins and promotes synapsis in the absence of an axial element in mammalian meiotic cells. *Mol. Cell. Biol.* 21:5667–5677.

Peters, A.H., A.W. Plug, M.J. van Vugt, and P. de Boer. 1997. A drying-down technique for the spreading of mammalian meiocytes from the male and female germline. *Chromosome Res.* 5:66–68.

Prieto, I., J.A. Suja, N. Pezzi, L. Kremer, A.C. Martinez, J.S. Rufas, and J.L. Barbero. 2001. Mammalian STAG3 is a cohesin specific to sister chromatid arms in meiosis I. *Nat. Cell Biol.* 3:761–766.

Roeder, G.S. 1997. Meiotic chromosomes: it takes two to tango. *Genes Dev.* 11:2600–2621.

Schalk, J.A., A.J. Dietrich, A.C. Vink, H.H. Offenberg, M. van Aalderen, and C. Heyting. 1998. Localization of SCP2 and SCP3 protein molecules within synaptonemal complexes of the rat. *Chromosoma*. 107:540–548.

Schalk, J.A., H.H. Offenberg, E. Peters, N.P. Groot, J.M. Hoovers, and C. Heyting. 1999. Isolation and characterization of the human SCP2 cDNA and chromosomal localization of the gene. *Mamm. Genome*. 10:642–644.

Scherthan, H., S. Weich, H. Schwegler, C. Heyting, M. Harle, and T. Cremer. 1996. Centromere and telomere movements during early meiotic prophase of mouse and man are associated with the onset of chromosome pairing. *J. Cell Biol.* 134:1109–1125.

Schmekel, K., R.L. Meuwissen, A.J. Dietrich, A.C. Vink, J. van Marle, H. van Veen, and C. Heyting. 1996. Organization of SCP1 protein molecules within synaptonemal complexes of the rat. *Exp. Cell Res.* 226:20–30.

Smith, A.V., and G.S. Roeder. 1997. The yeast Red1 protein localizes to the cores of meiotic chromosomes. *J. Cell Biol.* 136:957–967.

Sym, M., J.A. Engebrecht, and G.S. Roeder. 1993. ZIP1 is a synaptonemal complex protein required for meiotic chromosome synapsis. *Cell*. 72:365–378.

Tarsounas, M., R.E. Pearlman, P.J. Gasser, M.S. Park, and P.B. Moens. 1997. Protein-protein interactions in the synaptonemal complex. *Mol. Biol. Cell*. 8:1405–1414.

Tarsounas, M., T. Morita, R.E. Pearlman, and P.B. Moens. 1999. RAD51 and DMC1 form mixed complexes associated with mouse meiotic chromosome cores and synaptonemal complexes. *J. Cell Biol.* 147:207–220.

von Wettstein, D., S.W. Rasmussen, and P.B. Holm. 1984. The synaptonemal complex in genetic segregation. *Annu. Rev. Genet.* 18:331–413.

Wang, P.J., and D.C. Page. 2002. Functional substitution for $TAF_{II}250$ by a retroposed homolog that is expressed in human spermatogenesis. *Hum. Mol. Genet.* 11:2341–2346.

Wang, P.J., J.R. McCarrey, F. Yang, and D.C. Page. 2001. An abundance of X-linked genes expressed in spermatogonia. *Nat. Genet.* 27:422–426.

Yang, Z., G.I. Gallicano, Q.C. Yu, and E. Fuchs. 1997. An unexpected localization of basonuclin in the centrosome, mitochondria, and acrosome of developing spermatids. *J. Cell Biol.* 137:657–669.

Yuan, L., J. Pelttari, E. Brundell, B. Bjorkroth, J. Zhao, J.G. Liu, H. Brismar, B. Daneholt, and C. Hoog. 1998. The synaptonemal complex protein SCP3 can form multistranded, cross-striated fibers in vivo. *J. Cell Biol.* 142:331–339.

Yuan, L., J.G. Liu, J. Zhao, E. Brundell, B. Daneholt, and C. Hoog. 2000. The murine SCP3 gene is required for synaptonemal complex assembly, chromosome synapsis, and male fertility. *Mol. Cell*. 5:73–83.

Yuan, L., J.G. Liu, M.R. Hoja, J. Wilbertz, K. Nordqvist, and C. Hoog. 2002. Female germ cell aneuploidy and embryo death in mice lacking the meiosis-specific protein SCP3. *Science*. 296:1115–1118.